

Effect of Accelerated Weathering on Color and Physico-mechanical Properties of Wood-plastic Composites with Nano Titanium Dioxide

Seyyed Khalil HosseiniHashemi  ^{a,*} Ahad Rahimi, ^a and Nadir Ayrilmis  ^{b,*}

Polypropylene (PP) with black locust wood flour and maleic grafted polypropylene were used to prepare wood plastic composites (WPC) by injection molding. The effect of the addition of nano titanium oxide (nano TiO_2) on the properties of the composites was investigated. The specimens were weathered in an accelerated weathering apparatus using a xenon arc lamp for 2000 h. The physical properties of the composites were evaluated by colorimetry, water absorption, and thickness swelling before and after weathering. Mechanical properties of WPC were also determined before and after weathering. The WPC containing 0.75 phr nano TiO_2 showed an improvement in the flexural and tensile strength and flexural and tensile modulus while the WPCs containing 0.2 phr nano TiO_2 showed an improvement in the impact strength. The UV resistance of the WPCs also improved with the incorporation of nano TiO_2 powder into the composites. Both water absorption and thickness swelling were found to be reduced by the incorporation of nano TiO_2 into WPC.

DOI: 10.15376/biores.20.1.1200-1213

Keywords: WPC; Nano TiO_2 ; Weathering; Mechanical properties; Water absorption; FTIR

Contact information: a: Department of Wood Science and Paper Technology, Karaj Branch, Islamic Azad University, Karaj, Iran; b: Department of Wood Mechanics and Technology, Forestry Faculty, Istanbul University-Cerrahpasa, Bahcekoy, Sariyer, 34473, Istanbul, Turkey;

*Corresponding authors: sk.hashemi@iau.ac.ir; nadiray@istanbul.edu.tr

INTRODUCTION

Wood-plastic composites (WPCs) have emerged as versatile and dynamic materials in the construction industry. They are produced by mixing wood particles into molten plastic, together with coupling agents or additives, to form composite materials through processes such as extrusion, compression, or injection molding. The origins of WPCs can be traced back to 1983, when the American company Woodstock pioneered their production for automotive interiors using extrusion technology, combining polypropylene with wood flour. Since then, global production and market demand for WPCs has grown exponentially. In North America, for example, the market share of WPC flooring components rose from 2% by weight in 1997 to around 18% in 2005, reaching a significant \$3.9 billion in the residential, commercial and fencing sectors (Smith and Wolcott 2006). WPCs are mainly used in construction applications such as flooring, fencing, shelters, garden furniture, exterior windows, and doors (Smith and Wolcott 2006). They are also used in a wide range of sectors including the marine industry, railways, automotive components, and highway infrastructure such as signs, guard posts, and fence posts (Youngquist *et al.* 1994). Compared to pure polymers,

WPCs exhibit improved mechanical properties, thermal stability, and resistance to UV light and degradation (Optimat and Merl 2003). Despite advances in the production of WPCs, concerns remain about their performance in outdoor environments.

Exposure of WPC to moisture, heat and UV light during use accelerates the physical degradation and biological decomposition of both its wood and polymer components. The extent of degradation depends on factors such as moisture content and temperature, which can significantly affect the physical and mechanical properties of WPCs (Marcovich *et al.* 1998; Lin *et al.* 2002). Exposure to UV light induces changes in the wood surface, altering its physical and mechanical properties through color changes and degradation of lignin (Pandey 2005). In addition, WPCs are susceptible to photodegradation when exposed to UV radiation (Gijsman *et al.* 1999; Gulmine *et al.* 2003). Aydemir *et al.* (2016a) investigated the preparation of a polymer composite from polypropylene and nano titanium dioxide (TiO_2 , from 0.5 to 4 wt%) using extrusion/injection molding method. The effect of the amount of the TiO_2 on the water absorption, strength, and crystallization behavior of the polypropylene composites was investigated. The mechanical properties, except for the tensile modulus and impact strength, improved with the addition of the TiO_2 . When the TiO_2 was added in the range of 0 to 4 wt%, the addition of nano- TiO_2 slightly improved the thermal stability of the polypropylene. A similar result was also reported by Kaymakçı (2019). Kaymakçı stated that the thermal stability and mechanical properties (tensile and flexural properties) of WPCs improved as the amount of the TiO_2 increased from 1 to 5%.

TiO_2 has many electrical, optical, and chemical properties. It is a high-performance material. Ultraviolet radiation is the radiation from sunlight in the wavelength range of 100 to 400 nanometres (nm). TiO_2 particles are used in composite materials because of their high ability to absorb UV radiation. The main advantages of the TiO_2 pigments used in coating applications are excellent hiding power, high chemical stability, high refractive index, and high weather resistance (Li *et al.* 2024).

In the field of materials science, the integration of nanotechnology has attracted considerable interest from both scientific and industrial sectors, particularly in the reinforcement of polymers with nanofillers (Kaffashi *et al.* 2007). The primary objective of this study was to investigate various physical, mechanical, and chemical properties of a hybrid composite of wood flour, polypropylene, and nanofillers after exposure to accelerated weathering.

EXPERIMENTAL

Materials

To produce black locust flour (BWF), the branches of the black locust plant (*Robinia pseudoacacia* L.) were first cut into small pieces and then ground in a laboratory mill (Wieser, model: WGLS 200/200). The flour had a particle size that varied between 40 and 60 mesh. The BWF was then subjected to a drying process in an oven set at 103 ± 2 °C for 24 h to obtain a moisture content between 0% and 1%. Empty plastic bags were used to store the material until it was mixed with polypropylene (PP).

Table 1. Compositions of the WPC Formulations

Specimen Code	PP (wt%)	Wood Flour (wt%)	Nano TiO ₂ (phr)	MAPP (phr)
Control	40	60	0	2
0.20 nano TiO ₂	40	60	0.2	2
0.50 nano TiO ₂	40	60	0.5	2
0.75 nano TiO ₂	40	60	0.75	2
1.00 nano TiO ₂	40	60	1	2

The homopolymer polypropylene (PP, code: P10800) was supplied by Arak Petrochemical Company, Arak city, Iran, and had a melt flow rate between 7 and 10 g/10 min when heated to 190 °C. Maleic anhydride grafted polypropylene (MAPP) was supplied by Alderich Company (code: 427845; Alderich, Germany) and was used as the coupling agent. Table 1 shows the premixed components of each WPC formulation.

Preparation of Injection Molded Biocomposite Specimens

The wood flour, the polypropylene, and the nano-TiO₂ were mixed together by dispersion using a mixer. The pre-blended components were fed through a Dr Collin System counter-rotating twin screw extruder (Sportparkstr. 2, D-85560 Ebersberg, Germany) operating at a temperature of 180 °C and a screw speed of 60 rpm. After extrusion, the combined material was cooled in water and then pelletized. Before injection, these pellets were dried at 85 °C for 24 h. Finally, an injection moulding machine (Imen Machine Company, Tehran, Iran) was used at temperatures between 180 and 190 °C and a pressure of 10 MPa.

Test specimens were conditioned for a minimum of 40 hours at 23 °C and 50% relative humidity prior to testing in accordance with ASTM D618 (2021). Notched impact strength was tested in accordance with ASTM D256 (2023) and flexural properties were evaluated in accordance with ASTM D790 (2017). Three specimens were used for each type of test.

Characterization Tests of Biocomposites

Colorimetry measurement

Color changes in the surfaces of the WPCs were measured during different periods of time (500, 1000, 1500, and 2000 h) using the method specified in ASTM D2244 (2016) standard. A BYK-Gardner Gloss 0.45 colorimeter (400 to 700 nm) (Itrak Company, Tabriz city, Iran) was used to measure color changes. The color coordinates for each composite were measured with five replicates before and after exposure in the accelerated weathering machine. Color changes were calculated using the following Eq. 1,

$$\Delta E = \sqrt{(L_2 - L_1)^2 + (a_2 - a_1)^2 + (b_2 - b_1)^2} \quad (1)$$

where index 1 corresponds to the value of the relevant factor before irradiation and index 2 corresponds to the value of the relevant factor after irradiation. According to the above-mentioned points, an increase in the L-factor means an increase in the brightness of the surface of the specimen, and an increase in the factor (a) means that the color of the surface of the specimen is red, and an increase in the factor (b) means that the color of the surface of the specimen changes to yellow.

FTIR (Fourier-transform infrared spectroscopy) analysis

FTIR spectroscopy (BRUKER Vertex-89 spectrometer, Massachusetts, USA) with Attenuated Total Reflectance (ATR-FTIR) was used to study the chemical changes in the functional groups of the WPC samples exposed to accelerated weathering. For each specimen, 16 scans were recorded in absorbance units from 4000 to 6000 cm^{-1} . The spectra were obtained using attenuated total reflectance (ATR).

Mechanical Properties

To ensure uniform temperature and humidity conditions and the absence of any influence of these factors (temperature, humidity, *etc.*) on the mechanical properties, the test specimens were placed in the conditioning room at 23 °C and 50% relative humidity for 48 h to reach equilibrium with the ambient humidity and temperature. The mechanical properties of the composites were measured according to ASTM guidelines and with 3 replicates.

Tensile tests were performed on the specimens in accordance with ASTM D638 (2022). The specimens were of the dumbbell type and the loading speed was 5 mm/min. An INSTRON model 4486 instrument (Frank Bacon Machinery Sales Co., MI, USA) was used to perform the test. The computer connected to the instrument provided information, such as resistance (MPa), modulus of elasticity (MPa), change in length at break (%), maximum load (kN), and similar information after the test for each treatment. To perform the tensile test, the appropriate jaws were mounted on the fixture and the strain gauge was attached to the specimen using special metal clamps.

Water Resistance

Physical properties, including water absorption and thickness expansion, and mechanical properties, including tensile strength of weathered specimens were measured after 2000 h of exposure to xenon lamps. The colorimetric test was carried out after 500, 1000, 1500, and 2000 h of weathering. This means that the specimens were subjected to a colorimetric test at each of these time periods. In addition, to further examine the surface of the specimens, after reaching each time point, the specimens were removed from the machine and then subjected to Fourier Transform Infrared (FTIR) testing (Spectrum-100D; PerkinElmer, Fremont, CA, USA).

Weathering Test

A similar approach to the arc-xenon irradiation method for plastics in outdoor applications, the accelerated xenon lamp weathering test followed the ASTM D2565 (2016) standard procedure. To perform this test, a xenon arc lamp with a filter is often placed in the centre of the ventilation chamber. This cylinder is rotated at a speed of one minute. It is common practice to expose weathering materials to the sun for 102 minutes and then spray them with water for 18 minutes. The optimum irradiance is 41.5 W/m^2 at wavelengths of 300 to 400 nm. A temperature of 63 °C and a humidity of 50% are maintained on the black panel during the exposure intervals.

Statistical Analysis

An analysis of variance, ANOVA, was performed ($p < 0.05$) to evaluate the effect of the accelerated weathering on the properties of the WPCs containing different amounts of the TiO_2 . Duncan's multiple range test was used to detect significant differences

between the means of the WPC types. Statistical analysis was performed using the IBM SPSS statistical program (version 19, IBM, Armonk, NY, USA).

RESULTS AND DISCUSSION

FTIR Analysis

The FTIR spectra of all the groups of WPCs treated with and without nano-TiO₂ are shown in Fig. 1. The structural changes occurred in the weathered WPCs were compared with the untreated control group. Spectral analysis of the surface of the weathered WPCs revealed significant spectral changes. A sharp peak at 1725 cm⁻¹ with a shoulder at 1742 cm⁻¹, corresponding to hydrogen-bonded carboxylic acid and ester groups, was observed in the carbonyl region (1750 cm⁻¹ to 1710 cm⁻¹) (Stark and Matuana 2004). The increase in the amount of the TiO₂ increased the intensity of the characteristic peaks of the wood and polypropylene. Common bands in the spectra of wood, polypropylene, and nano-TiO₂ indicated that all the composites were chemically identical. A similar result was observed in the WPCs containing iron oxide nanoparticles by Durmaz *et al.* (2024). They reported that ATR-FTIR analysis revealed almost no change in the characteristic bands of polymer (2916 cm⁻¹ and 2846 cm⁻¹) and wood (1512 cm⁻¹). The Ti-O-Ti stretching of TiO₂ is responsible for the high absorbance found in the region between 1028 and 418 cm⁻¹, according to Deka and Maji (2011). The band intensities of the TiO₂ bands increased with increasing nano-TiO₂ concentration. The following bands are associated with different chemical bonds: -OH stretching (mostly found in cellulose) at around 3400 cm⁻¹, -CH stretching at 2975 and 2721 cm⁻¹, C=O stretching at 1731 cm⁻¹ (mostly in lignin), -OH bending at 1638 cm⁻¹, C-O stretching at 1162 and 1046 cm⁻¹ (mostly in cellulose and hemicellulose), and C-H bending vibrations (out of plane) at 1000 to 650 cm⁻¹ (in wood flour). Possibly due to the nano-TiO₂ coating on the wood flour, the intensity of the band around 3400 cm⁻¹ decreased significantly as the amount of nano-TiO₂ increased.

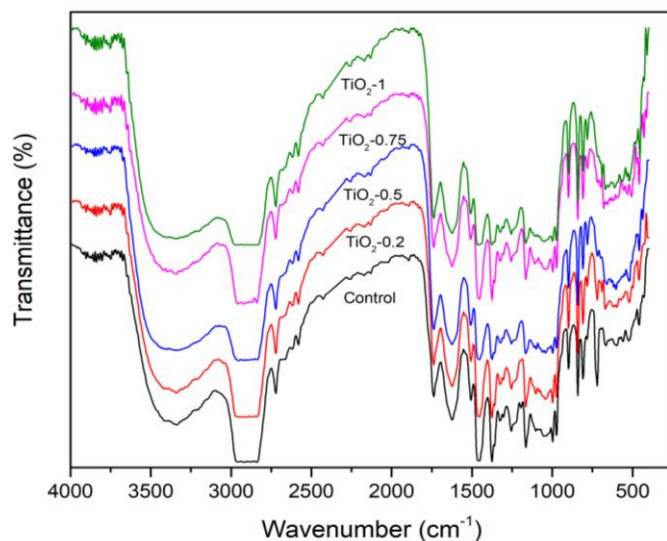


Fig. 1. The FTIR spectra of the biocomposites

Color Change of the WPCs

The values of the lightness (L), redness (a), and yellowness (b) factors were determined for each of the WPC specimens. Table 2 shows the average values of the color coordinates of all WPC specimens before weathering and after 500, 1000, 1500, and 2000 h of weathering. Table 2 also shows the average values of the changes in color coordinates and the total color change of the specimens after 500, 1000, 1500, and 2000 h of weathering.

The results of the analysis of variance show that the independent effect of nano-TiO₂ on the brightness change of WPC after 500 h of weathering resulted in a significant difference at the 95% confidence level. As shown in Table 2, by increasing the amount of nano-TiO₂ from 0 phr to 1 phr by weight increased the brightness change of the WPC increases after 500 h of weathering. The highest amount of the light changes related to the use of 1 phr by weight of nano-TiO₂ was equal to 35.9 and the lowest amount of change related to the use of 0 phr by weight of nano-TiO₂ was equal to 29.6.

Table 2. Mean Values of Color Coordinates and Total Color of Nano Composites Before and After Accelerated Weathering Test (500, 1000, 1500, and 2000 h)

Weathering Time (h)	Color Coordinates And Total Color	0 phr Nano TiO ₂	0.2 phr Nano TiO ₂	0.5 phr Nano TiO ₂	0.75 phr Nano TiO ₂	1 phr Nano TiO ₂
0	L	25.71	30.78	31.39	35.58	37.54
	a	6.63	5.72	8.80	8.33	7.37
	b	3.98	10.71	8.87	6.42	6.81
500	L	29.66	30.37	33.65	34.75	35.93
	a	6.15	6.15	6.24	6.22	5.95
	b	16.20	15.28	16.20	14.80	14.05
	ΔL	3.95	-0.41	2.26	-0.83	-1.61
	Δa	-0.48	0.43	-2.56	-2.11	-1.42
	Δb	12.22	4.57	7.33	8.38	7.24
	ΔE	6.74	2.04	4.45	4.59	4.13
1000	L	30.15	31.55	34.22	35.80	36.90
	a	7.40	7.40	7.30	7.50	6.50
	b	17.30	16.80	17.20	15.60	15.33
	ΔL	4.44	0.77	2.83	0.22	-0.64
	Δa	0.77	1.68	-1.5	-0.83	-0.87
	Δb	13.32	6.09	8.33	9.18	8.52
	ΔE	7.86	3.45	5.60	5.88	5.23
1500	L	32.66	33.50	34.27	37.23	38.76
	a	9.39	9.41	11.35	9.66	8.01
	b	19.13	18.22	11.90	17.50	11.34
	ΔL	6.95	2.72	2.88	1.65	1.22
	Δa	2.76	3.69	2.55	1.33	0.64
	Δb	15.15	7.51	3.03	11.08	4.53
	ΔE	9.67	5.12	7.51	7.71	2.87
2000	L	33.52	34.55	37.65	37.60	39.44
	a	10.41	10.20	10.34	10.33	9.77
	b	20.33	19.25	20.66	18.99	18.62
	ΔL	7.81	3.77	6.26	2.02	1.9
	Δa	3.78	4.48	1.54	2	2.4
	Δb	16.35	8.54	11.79	12.57	11.81
	ΔE	10.76	6.11	8.56	8.85	8.25

The results of the analysis of variance show that the effect of nano-TiO₂ on the brightness change of the WPC was not significant at the 95% confidence level. However, as shown in Table 2, the highest amount of brightness change (36) is related to composite specimens without nano-TiO₂ and the lowest amount was related to the use of 0 phr by weight of nano-TiO₂ equal to 30.

Given the data from the growth of carbonyl and vinyl groups, it was predicted that crystallinity would increase as a result of the chain breaking that occurred throughout the irradiation process. Kaci *et al.* (2001) used FTIR to investigate the crystallinity of light polyethylene after exposure to natural weathering. They observed that the crystallinity increased with increasing exposure time until it became stable after 400 days. They attributed this to secondary crystallinity in the amorphous phase, which they found to be the cause of this phenomenon. Durmaz *et al.* (2023) investigated the effect of nano zinc oxide nanoparticles on the weathering performance of wood-plastic composites. They reported that the control specimens exposed for 840 hours showed the highest colour changes (ΔE^*). The UV resistance was improved and colour changes were reduced by adding zinc oxide nanoparticles.

Mechanical Properties

When analysing the effect of the TiO₂ on the flexural strength of composites, it was found that the flexural strength of composites improved as the amount of the TiO₂ increased (Fig. 2). In a previous study, Han *et al.* (2008) described this improvement in the filling of gaps between composite components by nanoparticles, resulting in an increase in the mechanical strength of the composite. In another study, Deka and Maji (2011) highlighted that the flexural and tensile properties of composites are improved when TiO₂ nanoparticles are systematically dispersed throughout the material. Researchers from different institutions have reported similar results (Saeed *et al.* 2009; Aydemir *et al.* 2016b; Wang *et al.* 2020). In contrast, the increase in flexural strength and modulus was not statistically significant when the maximum amount of the TiO₂ was used. The specimens with the highest concentration of the TiO₂ (1 phr) showed a slight reduction in flexural strength compared to those with 0.75 phr TiO₂.

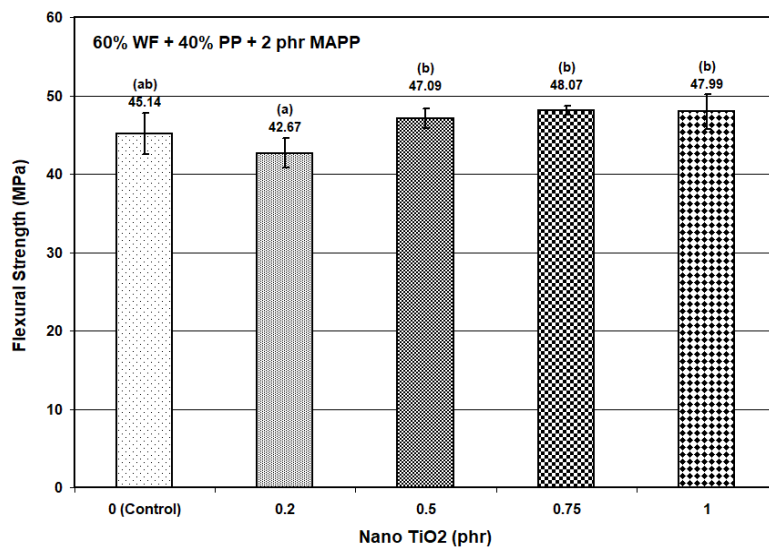


Fig. 2. The flexural strength of the biocomposites

This decrease is attributed to increased localized agglomeration, particularly at TiO_2 levels above 0.75 phr. However, beyond this concentration, subsequent additions resulted in a decrease in the modulus of elasticity (MOE). Due to their high surface energy, nanoparticles have a tendency to aggregate in an uncontrolled manner, a phenomenon known as agglomeration. Similar trends were observed in previous studies (Ashori and Nourbakhsh 2011; Deka and Maji 2011; Ghalehno *et al.* 2020).

The flexural modulus (MOE) of the composites showed an increase with TiO_2 loading up to 1 phr, but the increase was not statistically significant (Fig. 3).

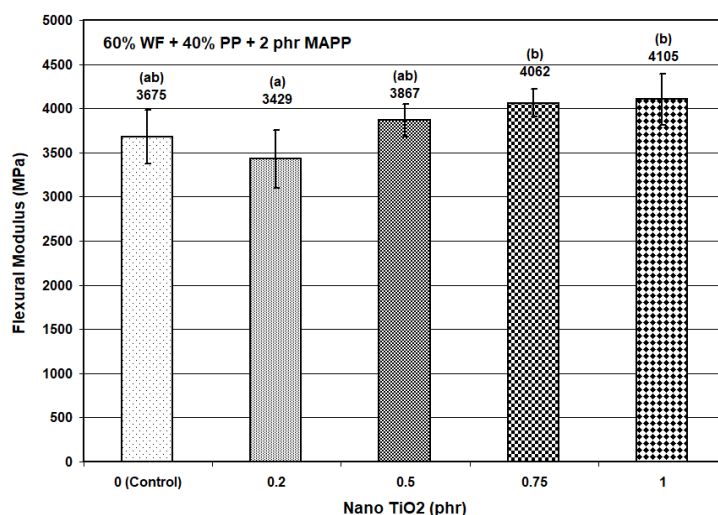


Fig. 3. The flexural modulus (MOE) of the biocomposites

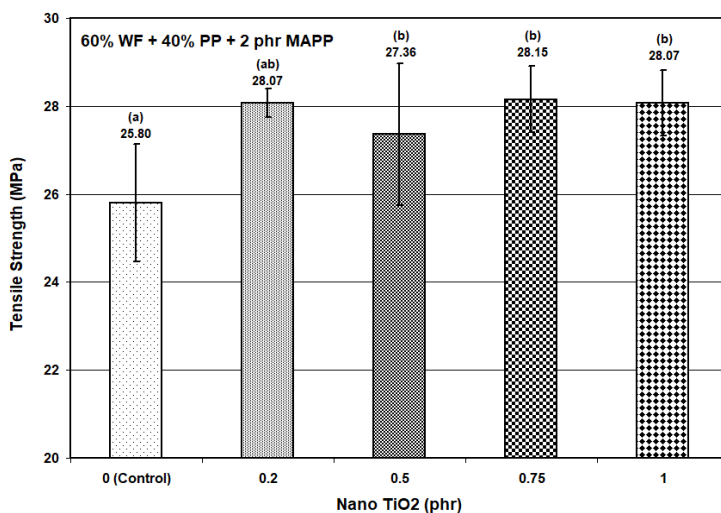


Fig. 4. The tensile strength of the biocomposites

The increase in the MOE of the WPCs with higher amount of the nano- TiO_2 can be explained by the improvement in the stress transfer from the polymer to the filler. Furthermore, in order to increase the adhesion between the wood flour and the polymer matrix, TiO_2 was able to promote interactions between these components. Compared to the control WPC without nanofillers, nano-WPCs showed better mechanical properties (Deka and Maji 2011; Kaymakci 2019).

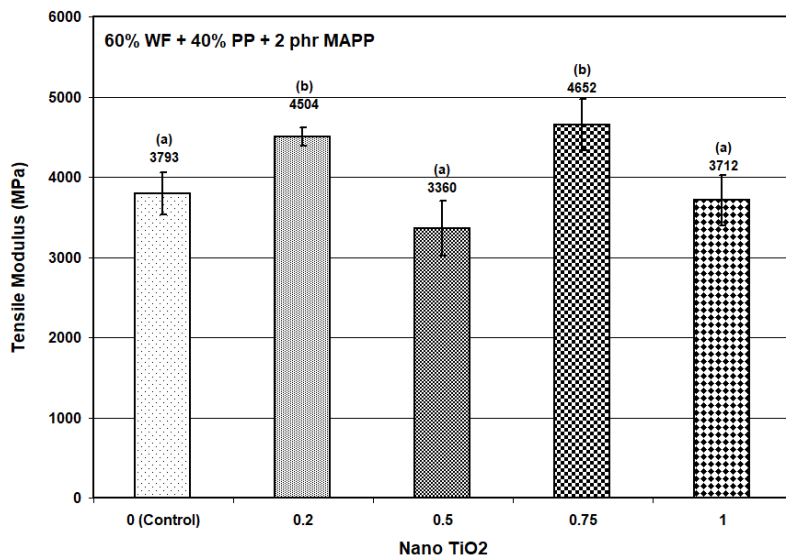


Fig. 5. The tensile modulus of the biocomposites

The results show that with increasing the nano-TiO₂, the tensile strength has improved almost constantly (Fig. 4). Aydemir *et al.* (2016a) reported that tensile strength, flexural strength, and the modulus of elasticity at bending improved with the addition of nano-TiO₂. As shown in Figure 5, the tensile modulus of the WPCs decreased at higher amount of the nano-TiO₂. Lee and Kim (2009) investigated the effect of the organoclay on the mechanical and thermal properties of WPCs. They reported that it was possible that clay migration towards the wood flour/polymer interface was responsible for the decrease in MOE values observed in nano-WPCs containing 4 wt% nanoclay. The izod impact strength of the WPCs decreased with increasing content of the nano-TiO₂ (Fig. 6).

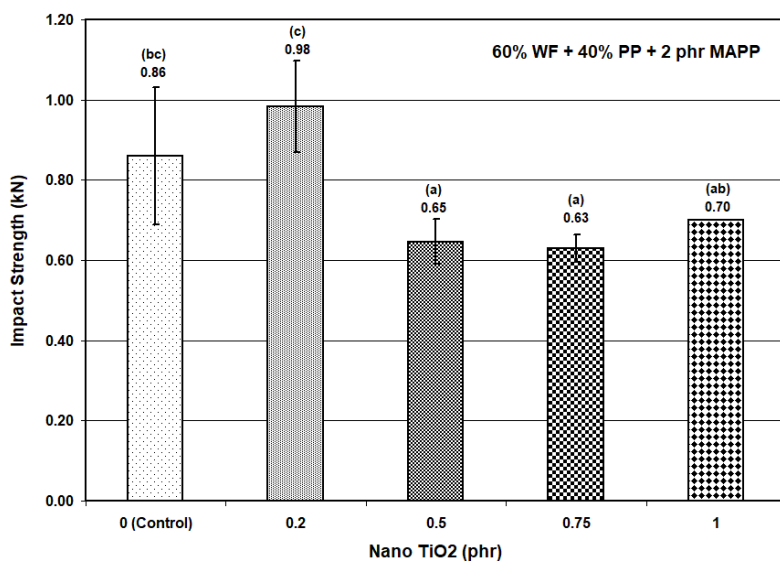


Fig. 6. The impact strength of the biocomposites

Water Resistance

In most cases, WPCs absorb more water when wood flour is used because of its hydrophilic properties. In the current study, the results of the water absorption and thickness swelling demonstrated that the TiO₂ effectively blocked water penetration in the WPC specimens. Similar results were found in a previous study (Kord *et al.* 2011). Additionally, the improvement in the water resistance of the WPCs can be also explained by the increased TiO₂ content that decreased the voids in the WPC, minimizing space available for water sorption (Abedini Najafabadi 2013). Both the tortuous path and reduced pore volume contribute to the lower water absorption capacity of the WPCs. Therefore, the nano-WPCs exhibited better water resistance as compared to the control WPCs. Devi and Maji (2012) investigated the effect of nano-ZnO addition on the water absorption of WPCs. According to their results, as the amount of nano-ZnO increased, the water absorption capacity decreased. The SEM analysis confirmed that the ZnO nano particles occupied the voids in the composites, and thus reduced the available space for water absorption. In other study, according to Samariha *et al.* (2015), there is a direct correlation between the amount of nanoclay present and the decrease in water absorption. According to Alexandre *et al.* (2006), nano filler (nano clay) reduced the water diffusivity by making the water transport pathway more complex. Aydemir *et al.* (2016b) reported that the water absorption of the composites with nano-TiO₂ was lower than that of the pure polypropylene. They attributed the decrease in water uptake to the hydrophobic properties of TiO₂. There was an increase in the water absorption of all the specimens as a result of the ageing process (Fig. 7). The WPCs increased by 26.1% and the nano-WPCs with 2% and 4% TiO₂ by weight increased 24.1% and 19.9%, respectively, when comparing the water absorption values before and after ageing. The thickness swelling results followed the same pattern as the water absorption results and are shown in Fig. 8.

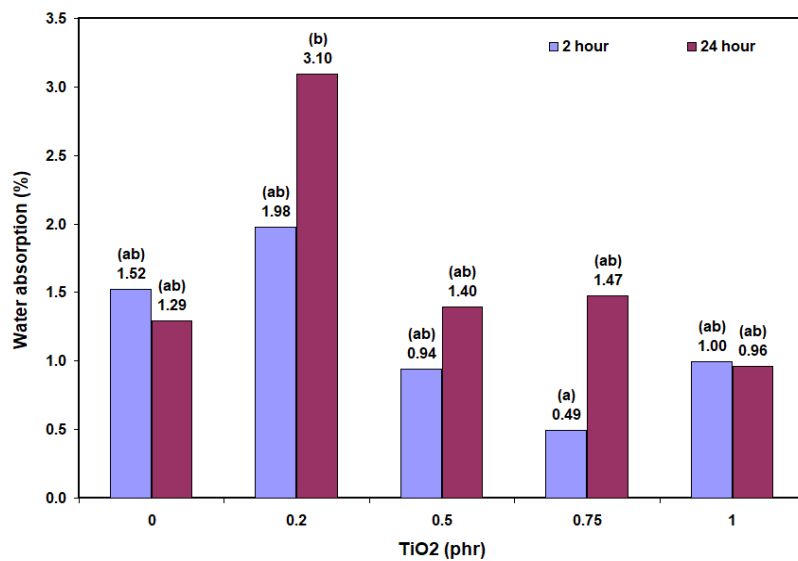


Fig. 7. The water absorption of the biocomposites

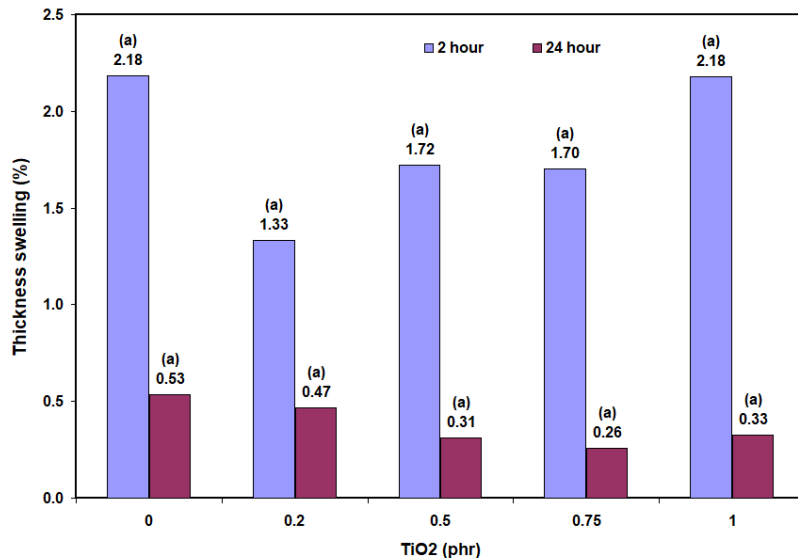


Fig. 8. The thickness swelling of the biocomposites

These results indicate that nano-WPCs were less affected by environmental factors than WPCs in terms of water absorption. Previous research showed that composites became more wettable under weathering conditions (Colom *et al.* 2003; Grigoriadou *et al.* 2011) and that the metal ions in the nanoparticles could accelerate the photodegradation of high-density polyethylene (HDPE). Therefore, it was expected that the WPCs with TiO₂ would degrade more rapidly when exposed to UV light, followed by an even greater increase in water absorption than the WPCs alone. However, the 0.2 phr nano-WPCs showed a small increase in water absorption compared to the WPCs. This could be due to agglomeration. These results were confirmed by other studies on the WPCs containing nano-TiO₂ (Kaymakci 2019; Aydemir *et al.* 2016b). Moreover, Eshraghi *et al.* (2013) found that nanoclays were more effective in reducing water absorption than in increasing degradation.

CONCLUSIONS

1. This study focused on investigating the water resistance, strength, and chemical properties of the wood flour, polypropylene, and nanofiller hybrid composites after exposure to accelerated weathering.
2. Based on the results, the wood-polymer composite (WPC) containing 0.75 phr nano-TiO₂ had better strength and modulus properties, but the WPC containing 0.2 phr nano-TiO₂ showed an improvement in the impact strength.
3. The UV resistance of the WPCs was improved by the addition of the nano-TiO₂ powder.
4. In addition, both water absorption and thickness swelling of the specimens decreased with the addition of the nano-TiO₂ to the WPC.
5. The decrease in the modulus of elasticity (MOE) after degradation was significantly less for nano-WPCs than for the WPCs. When all the test results were evaluated, it can be said that the optimum content for the nano-TiO₂ in the WPC was 0.75 phr.

ACKNOWLEDGMENTS

The authors wish to thank for the support of the Department of Wood Science and Paper Technology, Karaj Branch, Islamic Azad University.

REFERENCES CITED

Abedini Najafabadi, M. A., Nouri Khorasani, S., and Moftakharian Esfahani, J. (2014). "Water absorption behaviour and mechanical properties of high density polyethylene/pistachio shell flour nanocomposites in presence of two different UV stabilizers," *Polym. Polym. Compos.* 22(4), 409-416. DOI: 10.1177/096739111402200407

Alexandre, B., Marais, S., Langevin, S., Médéric, P., and Aubry, T. (2006). "Nanocomposite-based polyamide 12/montmorillonite: Relationships between structures and transport properties," *Desalination* 199(1-3), 164-166. DOI: 10.1016/j.desal.2006.03.035

Ashori, A., and Nourbakhsh, A. (2011). "Preparation and characterization of polypropylene/wood flour/nanoclay composites," *Eur. J. Wood Wood Prod.* 69(4), 663-666. DOI: 10.1007/s00107-010-0488-9

ASTM D256-23 (2023). "Standard test methods for determining the Izod pendulum impact resistance of plastics," ASTM International, West Conshohocken, PA, USA.

ASTM D618-21 (2021). "Standard practice for conditioning plastics," ASTM International, West Conshohocken, PA, USA.

ASTM D638-22 (2022). "Standard test method for tensile properties of plastics," ASTM International, West Conshohocken, PA, USA.

ASTM D790-17 (2017). "Standard test methods for flexural properties of unreinforced and reinforced plastics and electrical insulating materials," ASTM International, West Conshohocken, PA, USA.

ASTM D2244-16 (2016). "Standard practice for calculation of color tolerances and color differences from instrumentally measured color coordinates," ASTM International, West Conshohocken, PA, USA.

ASTM D2565-16 (2016). "Standard practice for xenon-arc exposure of plastics intended for outdoor applications," ASTM International, West Conshohocken, PA, USA.

Aydemir, D., Gumus, H., Yildiz, S., Gumus, S., Bardak, T., and Gunduz, G. (2016a). "Nanocomposites of polypropylene/nano titanium dioxide: Effect of loading rates of nano titanium dioxide," *Materials Sci.* 22(3), 364-369. DOI: 10.5755/j01.ms.22.3.8217.

Aydemir, D., Civi, B., Alsan, M., Can, A., Sivrikaya, H., Gunduz, G., and Wang, A. (2016b). "Mechanical, morphological and thermal properties of nano-boron nitride treated wood materials," *Maderas: Cien. Tecnol.* 18(1), 19-32. DOI: 10.4067/S0718-221X2016005000003

Colom, X., Carrillo, F., Nogues, F., and Garriga, P. (2003). "Structural analysis of photodegraded wood by means of FTIR spectroscopy," *Polym. Degrad. Stabil.* 80(3), 543-549. DOI: 10.1016/S0141-3910(03)00051-X

Deka, B. K., and Maji, T. K. (2011). "Effect of TiO₂ and nanoclay on the properties of wood polymer nanocomposite," *Compos. Part A- Appl. S.* 42(12), 2117-2125. DOI: 10.1016/j.compositesa.2011.09.023

HosseiniHashemi et al. (2025). "Nano TiO₂ biocomposite," *BioResources* 20(1), 1200-1213. 1211

Devi, R. R., and Maji, T. K. (2012). "Effect of Nano-ZnO on thermal, mechanical, UV stability, and other physical properties of wood polymer composites," *Ind. Eng. Chem. Res.* 51(10), 3870-3880. DOI: 10.1021/ie2018383

Durmaz, S., Keles, O. O., Aras, U., Erdil, Y. Z., and Mengeloglu, F. (2023) "The effect of zinc oxide nanoparticles on the weathering performance of wood-plastic composites," *Coloration Technol.* 139(4), 430-440. DOI: 10.1111/cote.12666

Durmaz, S., Keles, O. O., Aras, U., Avci, E., and Atar, I. (2024). "Improvement of weathering and thermal resistance of wood-plastic composites with iron oxide nanoparticles," *J. Thermoplas. Compos. Mater.* 37(3), 1050-1066. DOI: 10.1177/08927057231191460

Eshraghi, A., Khademieslam, H., Ghasemi, I., and Talaiepoor, M. (2013). "Effect of weathering on the properties of hybrid composite based on polyethylene, wood flour, and nanoclay," *BioResources* 8(1), 201-210. DOI: 10.15376/biores.8.1.201-210

Ghalehno, M. D., Kord, B., and Sheshkal, B. N. (2020). "Mechanical and physical properties of wood/polyethylene composite reinforced with TiO₂ nanoparticles," *Cerne* 26(4), 474-481. DOI: 10.1590/01047760202026042753

Gijsman, P., Meijers, G., and Vitarelli, G. (1999). "Comparison of the UV-degradation chemistry of polypropylene, polyethylene, polyamide 6 and polybutylene terephthalate," *Polym. Degrad. Stabil.* 65(3), 433-441. DOI: 10.1016/S0141-3910(99)00033-6

Grigoriadou, I., Paraskevopoulos, K. M., Chrissafis, K., Pavlidou, E., Stamkopoulos, T. G., and Bikaris, D. (2011). "Effect of different nanoparticles on HDPE UV stability," *Polym. Degrad. Stabil.* 96(1), 151-163. DOI: 10.1016/j.polymdegradstab.2010.10.001

Gulmine, J. V., Janissek, P. R., Heise, H. M., and Akcelrud, L. (2003). "Degradation profile of polyethylene after artificial accelerated weathering," *Polym. Degrad. Stabil.* 79(1), 385-397. DOI: 10.1016/S0141-3910(02)00338-5

Han, G., Lei, Y., Wu, Q., Kojima, Y., and Suzuki, S. (2008). "Bamboo-fiber filled high density polyethylene composites; effect of coupling treatment and nanoclay," *J. Polym. Enviro.* 16(2), 123-130. DOI: 10.1007/s10924-008-0094-7

Kaci, M., Sadoun, T., and Cimmino, S. (2001). "Crystallinity measurements of unstabilized and HALS-stabilized LDPE films exposed to natural weathering by FT-IR, DSC and WAXS analyses," *Int. J. Polym. Anal. Charact.* 6(5), 455-464. DOI: 10.1080/10236660108033961

Kaffashi, B., Poorsang, F., and Sonbolestan, S. E. (2007). "Preparation of polyurethane/clay nanocomposites: Investigating the dispersion of organoclays in PTMEG," *Iran. J. Polym. Sci. Technol.* 20(3), 247-255. DOI: 10.22063/jipst.2007.802

Kaymakci, A. (2019). "Effect of titanium dioxide on some mechanical, thermal, and surface properties of wood-plastic nanocomposites," *BioResources* 14(1), 1969-1979. DOI: 10.15376/biores.14.1.1969-1979

Kord, B., Hemmasi, A., and Ghasemi, I. (2011). "Properties of PP/wood flour/organomodified montmorillonite nanocomposites," *Wood Sci. Technol.* 45(1), 111-119. DOI: 10.1007/s00226-010-0309-7

Lee, H., and Kim, D. S. (2009). "Preparation and physical properties of wood/polypropylene/ clay nanocomposites," *Appl. Polym. Sci.* 111(6), 2769-2776. DOI: 10.1002/app.29331

Li, F., Chen, J., Niu, L., Zhang, Y., Rong, M., Wang, Y., Jiang, J., Li, X., and Zhang, Z. (2024). "Instant dispersion of titanium dioxide in waterborne coatings by pinning polyacrylate nanospheres," *Prog. Org. Coat.* 186, article 107957. DOI: 10.1016/j.porgcoat.2023.107957

Lin, Q., Zhou, X., and Dai, G. (2002). "Effect of hydrothermal environment on moisture absorption and mechanical properties of wood flour-filled polypropylene composites," *J. Appl. Polym. Sci.* 85(14), 2824-2832. DOI: 10.1002/app.10844

Marcovich, N. E., Reboreda, M. M., and Aranguren, M. I. (1998). "Dependence of the mechanical properties of wood flour-polymer composites on the moisture content," *J. Appl. Polym. Sci.* 68(13), 2069-2076. DOI: 10.1002/(SICI)1097-4628(19980627)68:13%3C2069::AID-APP2%3E3.0.CO;2-A

Optimat, Ltd., and Merl, Ltd. (2003). "Wood plastic composites study - Technology and UK market opportunities," Research Report. Banburg, Oxon, United Kingdom. The Waste and Resource Action Programme. p: 1-100.

Pandey, K. K. (2005). "Study of the effect of photo-irradiation on the surface chemistry of wood," *Polym. Degrad. Stabil.* 90(1), 9-20. DOI: 10.1016/j.polymdegradstab.2005.02.009

Saeed, K. H., Park, S. Y., and Ali, N. (2009). "Characterization of poly(butylene terephthalate) electrospun nanofibers containing titanium oxide," *Iran. Polym. J.* 18(8), 671-677.

Samariha, A., Hemmasi, A. H., Ghasemi, I., Bazyar, B., and Nemati, M. (2015). "Effect of nanoclay contents on properties of bagasse flour/reprocessed high density polyethylene/nanoclay composites," *Maderas: Cienc. Tecnol.* 17(3), 637-646. DOI: 10.4067/S0718-221X2015005000056

Smith, P. M., and Wolcott, M. P. (2006). "Opportunities for wood/natural fiber-plastic composites in residential and industrial applications," *Forest Prod. J.* 56(3), 4-11.

Stark, N. M., and Matuana, L. M. (2004). "Surface chemistry changes of weathered HDPE/wood-flour composites studied by XPS and FTIR spectroscopy," *Polym. Degrad. Stabil.* 86(1), 1-9. DOI: 10.1016/j.polymdegradstab.2003.11.002

Wang, J., Zhang, W., Zhu, B., and Xiao, Y. (2020). "Microstructure and photocatalytic activity of TiO₂-SiO₂ composite materials," *J. Phys.- Conf. Ser.* 1676(1), article ID 012059. DOI: 10.1088/1742-6596/1676/1/012059

Youngquist, J. A., Myers, G. E., Muehl, J. H., Krzysik, A. M., Clemens, C. M., and Padella, F. (1994). *Composites From Recycled Wood and Plastics: A Project Summary*, Project Summary, USDA Forest Service, Forest Products Laboratory Madison, WI, USA.

Article submitted: October 11, 2024; Peer review completed: November 19, 2024;
Revised version received and accepted: November 27, 2024; Published: December 6, 2024.

DOI: 10.15376/biores.20.1.1200-1213